PAPER

A flexible laser ultrasound transducer for Lamb wave-based structural health monitoring

View the article online for updates and enhancements.

A flexible laser ultrasound transducer for Lamb wave-based structural health monitoring

Xiaoxi Ding[1]**, Wei Li**[1]**, Jitao Xiong**[1]**, Yanfeng Shen**[2] (iD) **and Wenbin Huang**[1] (iD)

[1] State Key Lab of Mechanical Transmission, Chongqing University, Chongqing, People's Republic of China
[2] University of Michigan-Shanghai Jiao Tong University Joint Institute, Shanghai Jiao Tong University, Shanghai, People's Republic of China

E-mail: whuang@cqu.edu.cn

CrossMark

Abstract

Lamb waves are widely used in structural health monitoring (SHM) for plate-like structures. In this paper, a new and flexible ultrasonic transducer with a high photo-acoustic conversion efficiency was proposed by using candle soot nanoparticles (CSNPs) and polydimethylsiloxane (PDMS). Experimental results demonstrate that the developed transducer can generate a longitudinal wave with a short duration of 0.28 μs under the illumination of a nanosecond laser pulse. The amplitude of the excited longitudinal wave is 10 times that of the signal generated by the traditional laser ultrasound technique. Further, wedge-shape transducers were developed to excite Lamb waves in a 1.5-mm thick aluminum substrate by the oblique incidence method. The specific dA_0 and S_0 modes of the Lamb wave with the central frequency of 647 kHz were successfully excited in the aluminum plate. Based on the synthetic aperture focusing imaging technique, a delay-and-sum signal processing method was adopted for damage location in the plate by using the A_0 mode Lamb. A 3.5-mm defect was well imaged and the results demonstrate that the developed flexible photo-acoustic transducer can be a good alternative method for SHM.

Keywords laser ultrasonic transducer, photo-acoustic effect, Lamb waves, synthetic aperture focusing imaging, structural health monitoring

1. Introduction

Numerous health assessment techniques such as bulk wave ultrasonic, x-rays, infrared thermography and eddy current have been used effectively for structural health monitoring (SHM). However, the majority of these techniques tend to be slow and cumbersome, especially for the inspection of large structures (pipelines, marine, ships and aerospace) [1]. The guided waves ultrasonic testing potentially offers a great alternative solution to the conventional approach towards SHM. The guided wave has some unique properties as follows [2]: (a) the guided waves can realize long-distance detection with low energy loss; (b) they possess dispersive and multi-modal characteristics, and can identify and locate different types of defects by selecting the appropriate mode and frequency; (c) guided waves have wide inspection range and

good sensitivity; (d) guided wave-based SHM procedures are often simple and fast, and low cost. It is these advantages that make them widely used as detection signals in current SHM studies [3]. Senyurek [4] successfully detected two common damage defects on the wing slats of Boeing 737 aircraft through Lamb waves. Rucka [5] used the finite element analysis to simulate the failure caused by the bolting of the plate beam and beam on a railway bridge, and successfully detected these two damages by Lamb wave.

The excitation of the Lamb wave can be activated based on various physical effects, which can be categorized as contact and non-contact types. The contact type mainly includes the piezoelectric effect, and the non-contact type mainly includes laser ultrasonic and electromagnetic ultrasonic [6]. The piezoelectric transducer has the merits of high efficiency and predictive consistency in transmitting and receiving
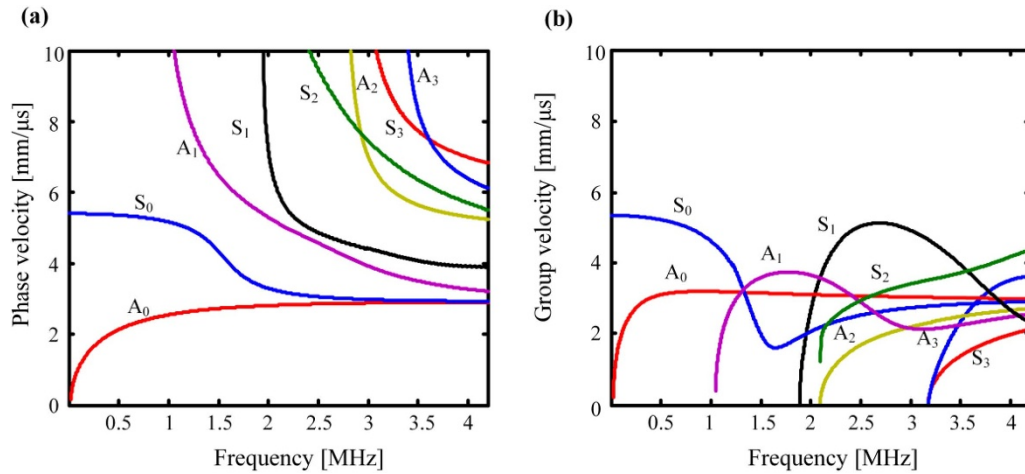
Figure 1. (a) Phase velocity and (b) group velocity dispersion curves of a 1.5 mm thickness aluminum plate.

ultrasonic Lamb waves. Attributed to the low cost and convenience for use, it provides a favorable approach for Lamb wave excitation [7, 8]. Non-contact excitation approaches mainly include electromagnetic ultrasonic and laser ultrasound. They have been widely applied for the applications where the direct contact between the transducer and the specimen is prohibited due to the harsh environment. The electromagnetic ultrasonic is an ideal choice for direct excitation and detection of horizontal shear waves, but it is limited to conductive material [9, 10]. On the other side, the laser ultrasonic technology has the characteristics of high energy, small light divergence angle, short duration, and can excite broadband guided signals [11, 12]. However, the conventional laser ultrasound suffers from two shortcomings. The application of traditional laser ultrasound in SHM is mainly to irradiate the laser directly on the surface of the tested sample, which results in low photo-acoustic conversion efficiency and requires high laser energy to excite the guide wave signal with high signal-to-noise ratio. Meanwhile, the mode and frequency of the excited Lamb wave by the conventional laser ultrasound is difficult to control, thus lacking the adaption for detecting different defects and structures.

Recently, a new type of composite laser ultrasound transducer was developed for achieving the high efficient laser-to-acoustic energy conversion. It comprises a laser absorption component and a thermal expansion component. The absorbed short-period laser pulse converts into the heat and then causes the thermal expansion. The short duration of the thermal expansion corresponds to an acoustic pulse propagating outward. Due to the high energy conversion efficiency and short duration of the laser pulse, the laser ultrasound transducer could generate a high-pressure acoustic signal with wide frequency bandwidth. Therefore, it has shown broad application prospects in bio-medical drug delivery, high-frequency ultrasound-focused targeted therapy, non-invasive high-precision surgery, and all-optical ultrasound imaging [13–15]. With respect to the imaging applications, Noimark [16] used multi-walled carbon nanotubes (MWCNT)–polydimethylsiloxane (PDMS) composites to coat optical fibers as all-optical acoustic transducers, achieving high ultrasonic pressure (peak-to-peak of 21.5 MPa) and broadband bandwidth (up to 39.8 MHz). In addition, high-resolution optical echo imaging of the aorta was obtained. However, reports about the Lamb wave excitation using this laser ultrasound transducer are still very limited.

In this paper, we described a new Lamb wave excitation technique by using a flexible laser ultrasonic transducer with high photo-acoustic conversion efficiency. The transducer is prepared from candle soot nanoparticles (CSNPs) and PDMS. The photo-acoustic performance was tested and compared with the conventional laser ultrasound technique. According to Snell's law, Lamb waves of the symmetric and asymmetric modes were excited in the aluminum plate by the oblique incidence of longitudinal waves. Finally, A_0 mode is selected for a damage detection demonstration using the synthetic aperture imaging technique. It is proved that this kind of flexible laser ultrasound transducer can be a good alternative for Lamb wave excitation in SHM applications.

2. Theory and methods of Lamb wave excitation

2.1. Theory of Lamb waves

Lamb waves, made up of a superposition of longitudinal and shear modes, are a form of elastic perturbation that can propagate independently in a thin plate. A Lamb mode can either be symmetric or anti-symmetric, which satisfies the wave equation and free boundary condition. The fundamental way to describe the propagation of Lamb modes in a particular material is with their dispersion curves, which plot the phase and group velocities versus the excitation frequency. Given the specific material property parameters, transducer dimension and excitation frequency, the Rayleigh-Lamb equation can be solved numerically to yield the dispersion curve [17]. The phase and group velocity dispersion curves for the different Lamb wave modes within a 1.5 mm thick aluminum plate are given in figure 1.
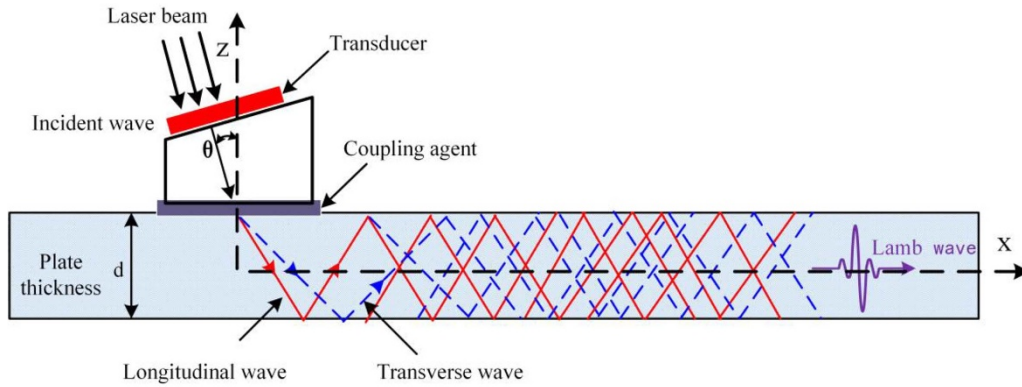
Figure 2. The Lamb wave excitation mechanism using the laser ultrasound transducer.

Lamb waves can be actively excited by a variety of means, including the piezoelectric ultrasonic probe, laser, electromagnetic acoustic transducer (EMAT), piezoelectric wafer active sensors (PWAS), and interdigital transducer, etc. An ideal Lamb mode for damage detection should possess the features including non-dispersion, low attenuation, easy excitability, single mode, good detectability, and high sensitivity. Based on these criteria, wedge-shaped transducers were developed to excite a Lamb wave in the 1.5 mm aluminum substrate by the oblique incident method. The oblique incidence of the longitudinal wave provides a precise and effective method for the excitation of the guided wave. When the longitudinal wave is incident at a certain angle, both the transverse and longitudinal wave modes will be excited in the substrate medium. The constructive interference of two waves will form a guided wave that travels horizontally along the wave guide, as shown in figure 2. To excite a certain Lamb wave mode with particular phase velocity at the excitation frequency, the incident angle of the laser can be calculated through Snell's law [18].

2.2. The basic principle of laser ultrasonic transducer

Laser-generated ultrasound provides an efficient way to transform laser energy into acoustic pulse without direct contact between the laser and the objective. The schematic diagram of the transducer can be seen in figure 3. The mechanism of laser generation of ultrasonic by the proposed transducer is based on the photo-acoustic effect [19]. The effect consists of two main procedures, i.e. the laser-heat conversion and thermal-acoustic transformation. The incident laser pulse is absorbed by a light absorption layer with high light extinction rate. The converted thermal energy promptly transfers to the surrounding thermal expansion materials to generate an acoustic pulse. By using a laser pulse with the duration of nanoseconds, a high-frequency ultrasound signal with a center frequency of tens of MHz can be readily excited [20].

Efficient laser transducers commonly have the following characteristics. First, the laser pulse duration is shorter than the thermal relaxation time, which confines the heat within the small irradiated volume [21]. Second, the pulse duration is shorter than the acoustical relaxation time [22]. Thus, by considering these prerequisites, the laser ultrasound pressure
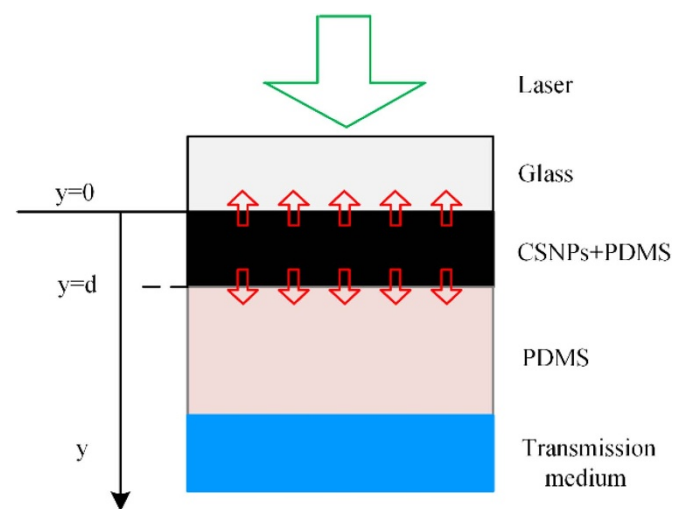

Figure 3. Schematic diagram of the laser ultrasonic transducer.

generated from a thin composite film can be simplified as:

$$P \cong \frac{\beta c}{C_p} \frac{E_{th}}{\tau}, \tag{1}$$

where β, c, C_p, E_{th} and τ denote the thermal expansion coefficient, the sound speed, the specific heat capacity, the converted thermal energy J/cm^2 and the laser pulse duration [23, 24].

This relation provides some obvious and meaningful instructions for the laser ultrasound materials selection. To achieve a high laser-acoustic energy conversion efficiency, the transducer material should have a high light absorption, a high thermal conduction rate and a large thermal expansion ratio. Previous works [25–28] have demonstrated that the mixture of black-colored carbon particles and PDMS can be a good material candidate for the laser ultrasound transducer. PDMS is favourable as the thermal expansion medium by virtue of its high thermal expansion coefficient ($\beta = 920 \times 10^{-6}$ K^{-1}) and optical transparency below the infrared band. Meanwhile, carbon nano-materials, e.g. carbon black (CB), carbon nano-fiber (CNF), carbon nanotube (CNT), and CSNPs have an excellent thermal conductivity [29], which is one of the main reasons
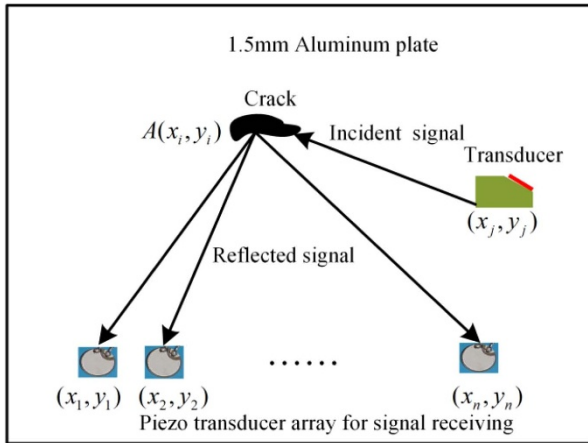
Figure 4. The synthetic aperture imaging method.

why carbon particles are commonly used as the light absorption materials for laser ultrasound transducers. Among these nanostructures, CSNPs have demonstrated the most superior performance, with a photo-acoustic energy conversion efficiency of 9.02×10^{-3}. This can be explained by their 3D nanoscale profile and chain-like structure, which provides a shorter thermal pathway to the surrounding PDMS medium. Therefore, CSNPs-PDMS was chosen as the material for the laser ultrasound transducer in this paper. It should be noted that the flexible nature of the transducer arises from the special material used. The CSNPs-PDMS composite and PDMS wedge has a low Young's modulus at MPa level. Also, it can withstand a 100% strain without breaking. Such a property made it very appropriate for the application of structures with complex geometry. However, to demonstrate the basic capability of the transducer for exciting the Lamb wave, we only examined the aluminum block and plate structures with flat profile in this paper.

2.3. Principle for the synthetic aperture focusing technique (SAFT)

The SAFT is a method for achieving high spatial resolution with high SNR in an ultrasound detection area [30, 31]. By employing a transducer array with a limited aperture for each single element, the effective aperture can be greatly enlarged, thus forming a smaller focusing zone and higher resolution, as shown in figure 4.

In the SAFT method, the defects reflect the incident Lamb wave pulse which could be received by all receiving elements. The time delay of each reflecting pulse depends on the relative distance between the defect and the receiving element. The SAFT method assumes that such reflecting pulse can be originated from any position with the same distance to the receiving element, which is equal to the multiple of time delay and the wave velocity. Therefore, the reflection magnitude at the position $A(x_i, y_i)$ can be back-calculated by summing all the contributions from each receiving element:

$$A(x_i, y_i) = \sum_{n=1}^{N} f_n(t_a), \tag{2}$$

where f_n is the received signal of the n_{th} receiving element, and *ta* is the time delay for the wave to travel from position A to the receiving element, which can be calculated as:

$$
\begin{aligned}
t_a &= t_{ij} + t_{in} \\
&= \frac{\sqrt{(x_j - x_i)^2 + (y_j - y_i)^2} + \sqrt{(x_n - x_i)^2 + (y_n - y_i)^2}}{c_g},
\end{aligned}
\tag{3}
$$

where c_g is the group velocity of the Lamb wave. (x_j, y_j) and (x_n, y_n) are the position for the exciting element and n_{th} receiving element.

3. Experimental methods

3.1. Fabrication of CSNPs-PDMS transducer

Figure 5 shows the fabrication processes of the CSNPs-PDMS laser ultrasound transducer. A rectangular high-temperature-resistant quartz glass with a size of 70 mm × 40 mm × 1 mm was used as the substrate of the laser ultrasound transducer. CSNPs were first grown on the first glass slide using a process called the flame synthesis method. The second glass slide was pre-coated with silane and then kept at room temperature for 6 h to make its surface anti-adhesive and uniform. The PDMS base and the curing agent (Sylgard 184) were mixed with a mass ratio of 10:1 and then placed in a vacuum container to degas for half an hour. The mixture was spin coated onto the top of the first glass slide with CSNPs. Then the second glass slide was placed on the first glass slide, which was coated with pre-cured PDMS. A 500 g weight was placed on two glass slides to provide a compression force. Attributed to the porous and branch-like structure of the candle soot (CS) layer, the pre-cured PDMS could penetrate into the CS layer and reach the first glass slide, which is the substrate of CSNPs. After the PDMS became fully cured under the 65 °C condition, the anti-adhesive glass slide could be removed and the PDMS layer was transferred onto the first glass slide with CS N Ps, thus forming the CSNPs-PDMS composite layer on the first glass slide. The CSNPs-PDMS composite layer covers about half of the slide and its thickness was measured to be about 100 μm by using a helical micrometer.

3.2. Characterization of the transducer

To illustrate the high photo-acoustic conversion efficiency of the new CSNPs-PDMS ultrasonic transducer, the performance of the laser ultrasound transducer for exciting the longitudinal wave in a 15 mm thick aluminum block was exanimated and compared with the direct laser radiation approach.

The experimental setup for the transducer characterization is shown in figure 6. A laser beam about 6 mm in diameter was excited by a 532 nm Q-switch Nd:YAG pulsed laser (CLASS-AI, Beijing Raycotech Optronic Corp) with a pulse duration of 6 ns and a 10 Hz repetition rate. The laser beam energy adjustment was conducted by an energy attenuator so as to ensure its stability. The laser beam has a diameter of 8 mm
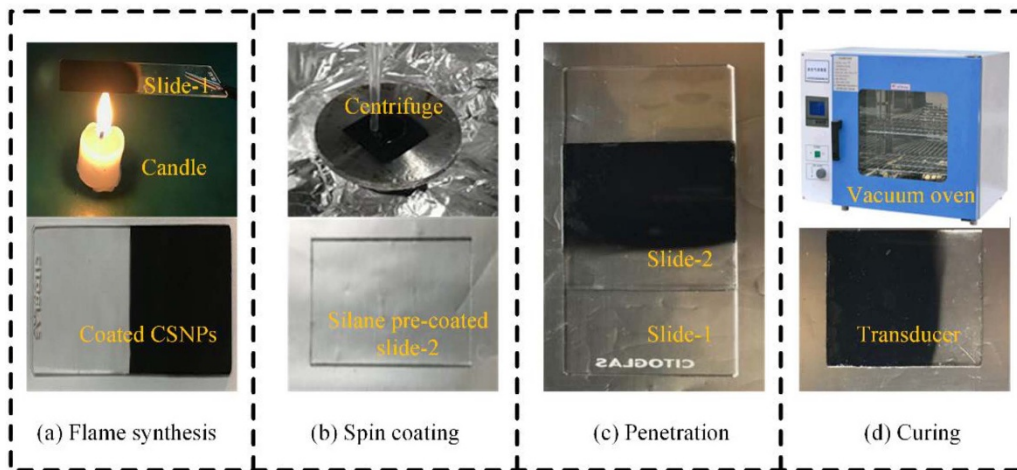
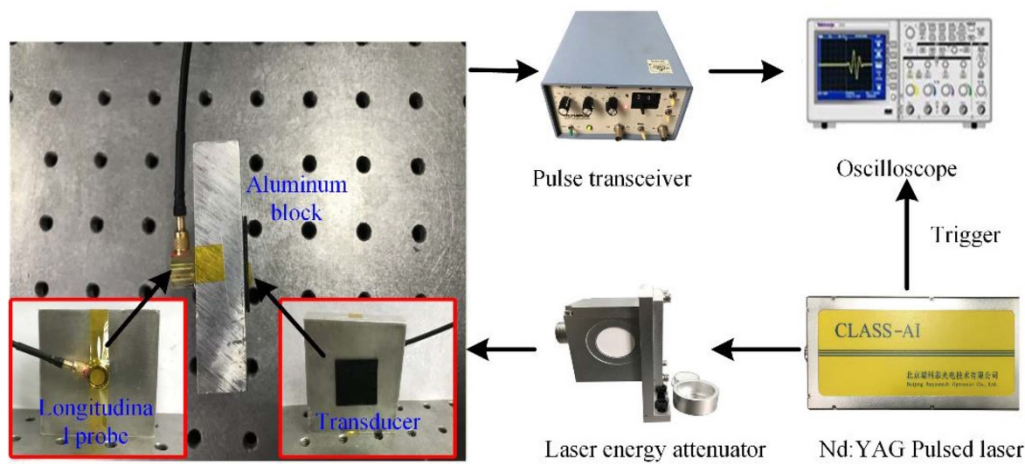**Figure 5.** The fabrication processes of CSNPs-PDMS transducer.

Figure 6. The experimental setup to characterize the transducer's performance for exciting the longitudinal wave in an aluminum block.

and is distributed in the form of Gaussian distribution over the surface of the transducer. The laser beam energy was measured by a pyroelectric energy sensor (PM100D, THORLABS). A longitudinal wave probe (DL10P6 L, Guangzhou Doppler Corp) with a diameter of 6 mm and a central frequency of 10 MHz was placed on the backside of the aluminum block by using an acoustic coupling gel to receive the longitudinal wave signal. The received signal was amplified by 20 dB using a pulse transceiver (5073PR, Olympus) and then recorded by a digital oscilloscope (TDS2024 C, Tektronix). Two sets of longitudinal wave excitation experiments of an aluminum block were performed. The first part was the excitation by the proposed transducer and the second part was the direct laser radiation excitation without using the transducer. To design the contrast experiment for demonstrating the effect of the transducer, no surface preparation of the aluminum block was conducted. Each waveform was obtained by averaging 16 signal traces in the time domain. The sampling frequency was chosen to be 2GS s^{-1}. The trigger signal was provided by the laser generator. The input laser energy was kept within 15 mJ to avoid damaging the transducer under excessive power.

3.3. Lamb wave excitation based on laser ultrasonic transducer

As the center frequency of acoustic pulse generated by a thin laser ultrasound transducer is above 10 MHz, it is too high for the Lamb wave excitation in a millimeter-thick metal plate. Since the high-frequency ultrasound has a much higher attenuation in the composite material, a thick transducer can be utilized for attaining an acoustic wave with the center frequency about hundreds of kHz. A 20 mm thick CSNPs-PDMS was fabricated and the excited longitudinal wave was recorded using a similar setup as shown in figure 6, but without using the aluminum block. A lower sampling frequency of 25 MS s^{-1} was used for data recording. In the longitudinal wave excitation, several batches of laser-acoustic transducers were prepared under the same experimental conditions and were investigated across a week. It is found that the amplitude, center frequency and bandwidth of the generated waveforms were almost consistent across batches, demonstrating the good repeatability of the transducer. The largest variations of the above parameters were measured to be 5%, 0.8% and 0.6% across a week, respectively. The center frequency was found
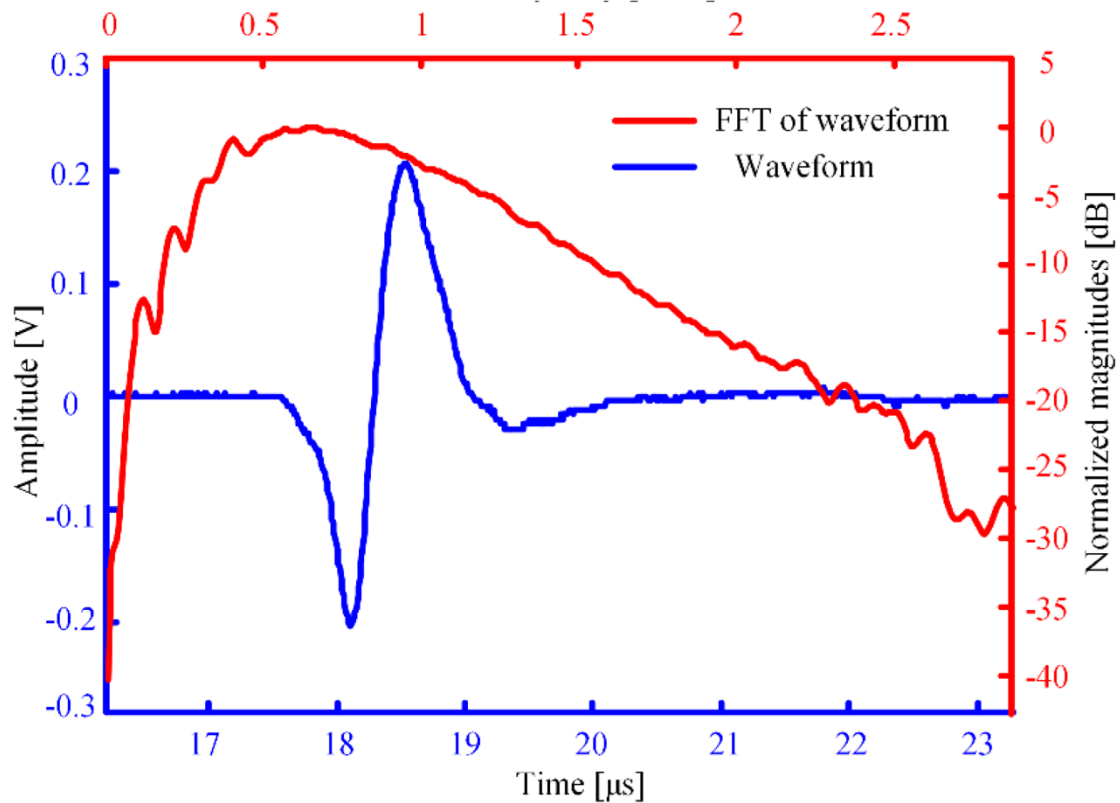
Figure 7. Longitudinal wave signal propagating in the thick CSNPs-PDMS composite.
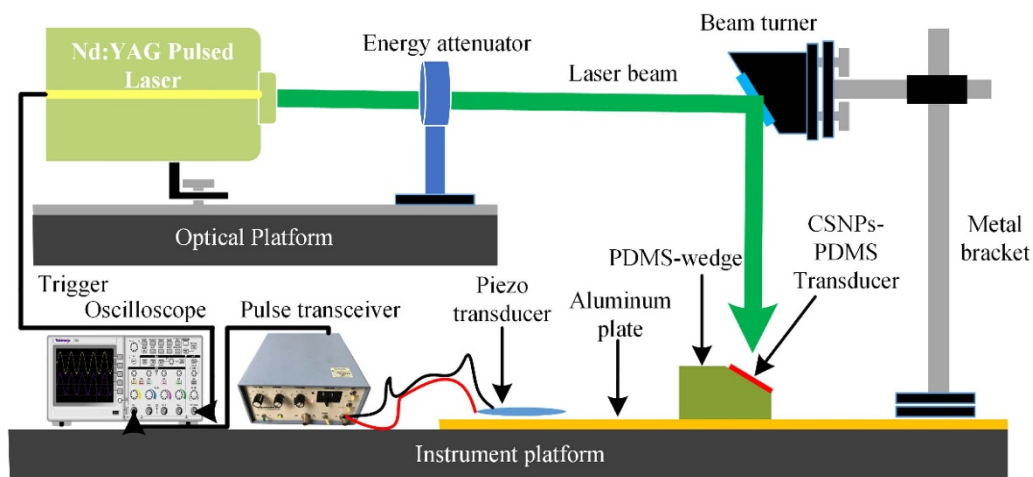

Figure 8. Schematic diagram of laser ultrasonic guided wave excitation experiment.

to be 647 kHz and the −3 dB bandwidth is 653 kHz, as shown in figure 7.

In order to excite the specific A_0 and S_0 modes of the Lamb wave and investigate its characteristics, corresponding experimental procedures were designed. The experimental setup of the laser ultrasonic guided waves excitation is shown in figure 8. To avoid the energy lost due to the reflections of sound waves at the transducer-air-substrate interfaces, a small amount of PDMS gel was used as a coupling agent. As the coupling agent has the same material composition with the wedge, a better transmission efficiency can be achieved. In

addition, the PDMS gel can be cured within 48 h under room temperature. Therefore, it can provide a permanent bonding of the transducer to the substrate if necessary. The laser source and the signal receiving instrument are similar to the longitudinal wave excitation experiment. The laser beam was irradiated upon the transducer after a 45-degree mirror. The diameter and distribution of the laser beam on the transducer are consistent with those used in the longitudinal wave excitation experiment. Wedge-shaped transducers were developed to excite Lamb wave in the 1.5-mm aluminum substrate by the oblique incidence method as mentioned in section 2. According to

Table 1. Wedge angles corresponding to different Lamb wave modes excitation.

Central Frequency	θ_{A_0}	θ_{S_0}
647 KHz	27°	11°

Snell's law and the central frequency of the longitudinal wave, oblique wedges with two different angles were designed to excite A_0 and S_0 mode Lamb waves, respectively. The details of the frequency and wedge angle is listed in the table 1. The critical incident angle of the A_0 mode (27°) calculated through Snell's law is much larger than that of the S_0 mode (11°) at 647 kHz. A circular PZT with a center frequency of 450 kHz was utilized as a receiver to detect Lamb wave signals generated by the wedge-shaped transducer before amplification. Each waveform was obtained by averaging 64 signal traces in the time domain and being denoised by a dB4 wavelet in the subsequent data processing procedure. The wavelet transform can decompose the original signal into multiple components with different wavelet coefficients by using the Mallat algorithm. The signal components with the wavelet coefficients below the given threshold are considered to be generated by noise, and can be set to zero to achieve the purpose of denoising [32].

3.4. Defect detection with the laser ultrasonic transducer

The experimental setup for the damage detection using the laser ultrasound transducer is shown in figure 9. An elliptical through thickness slit is prefabricated by using a grinding tool at the center of the aluminum plate with the size of 6×4 mm². Its geometry was not regular and had a rough margin. Its long side was almost along the horizontal line. A thick CSNPs-PDMS wedge transducer was used, with a diameter of 36 mm and a thickness of 20 mm, to excite the A_0 mode of Lamb wave for defect location. Similar to the previous longitudinal excitation experiment, a small amount of PDMS gel was applied as a coupling agent. The distance between the wedge and defect was set to be 70 mm. The wedge has an orientation of 45° and the projecting line of the wedge surface could reach the slit center. In this case, a better signal-to-noise ratio of the received scattered signal can be obtained. Nine piezoelectric sensor elements were placed as a linear array with the pitch of 8 mm. The center position of the array is set as the coordinate origin. The relative coordinate of the defect center is (−5 mm, 160 mm), corresponding to r = 160 mm and $\varphi = 92°$ in the polar coordinate. The signal collected from each receiving element are sent to the computer for further analysis.

4. Results and discussion

4.1. Excitation of the longitudinal wave

The acoustic signals generated with and without using the laser ultrasound transducer under a 5.1 mJ laser pulse are displayed in figure 10. Two signals have the time duration of 0.017 μs and 0.014 μs, respectively, with the center frequency
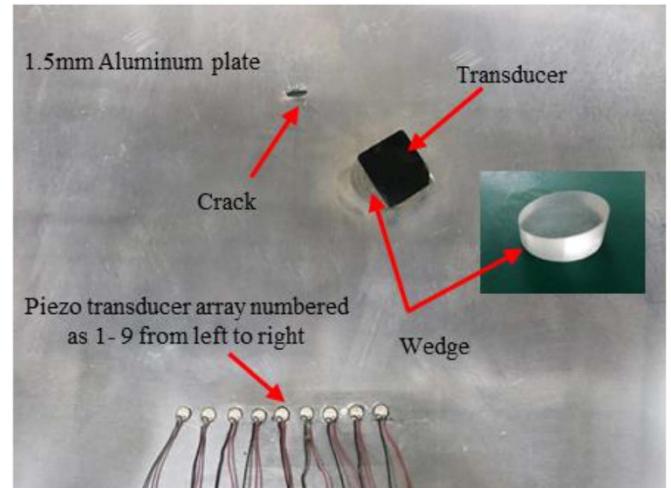
Figure 9. Experimental setup for crack imaging by the laser ultrasound transmitter and piezoelectric receiver array system.

of 19.68 MHz and −6 dB bandwidth of 13.89 MHz. It indicates that the laser ultrasound transducer causes little distortion to the acoustic signal. In addition, under the same laser energy excitation condition, the average amplitude of the excited longitudinal wave from the proposed transducer is 10 times that of the signal generated by direct laser exposure without using the transducer. This shows that the photo-acoustic conversion efficiency of the laser ultrasonic is greatly improved by using the proposed transducer.

The peak-to-peak amplitudes of the longitudinal wave signals with and without using the laser ultrasound transducer were plotted as a function of laser energy in figure 11. According to the experimental results, the amplitude of the longitudinal wave signal increases linearly with the laser energy within the entire investigation range for the direct radiation. However, for the laser ultrasound transducer, the longitudinal wave signal climbs linearly with the laser energy at low energy level but becomes saturated above 10 mJ. This is because that the nonlinear phenomena occur within the laser ultrasound transducer. This phenomenon is in accordance with our previous publication [27]. The linkage between the CSNPs with the PDMS can be destroyed by the strong thermal expansion, thus cutting the path for heat transfer. Meanwhile, the adhesion between the composite and the substrate can be damaged, which leads to the creation of an air gap in between and prohibits the transmission of the acoustic wave. For the Lamb wave excitation and imaging experiment, a 5.1 mJ laser pulse was used, ensuring that the transducer would remain in the thermoelastic regime.

4.2. Excitation of A_0 and S_0 mode Lamb wave

Figure 12 shows the excitation effect of the wedge laser ultrasonic transducer on A_0 and S_0. The signal waveform is received by the PZT sensor at the distance of 200 mm. Due to the numerous reflection of the longitudinal and transverse waves within the plate, a dispersive Lamb wave packet can be formed. In figure 12(a), there is only one distinct wave packet with a
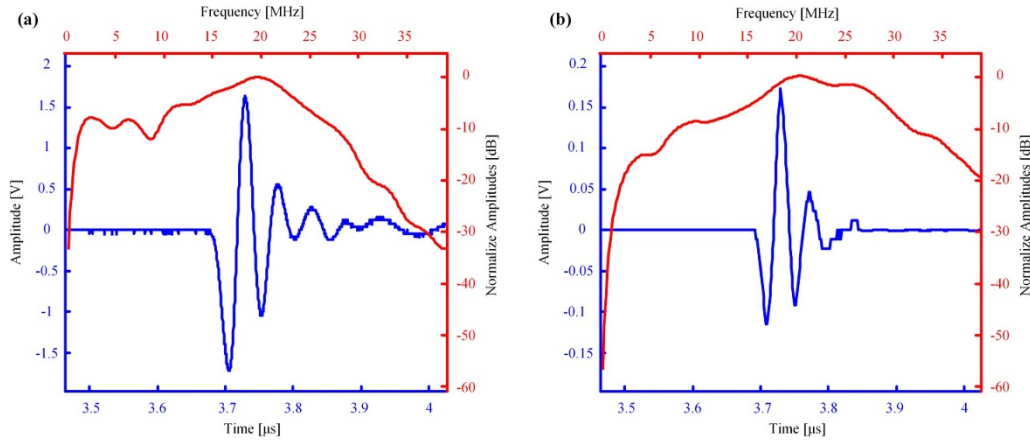
Figure 10. Comparison of the longitudinal wave signals in a 15 mm thick aluminum block excited by a 5.1 mJ laser pulse (a) with and (b) without the laser ultrasound transducer.
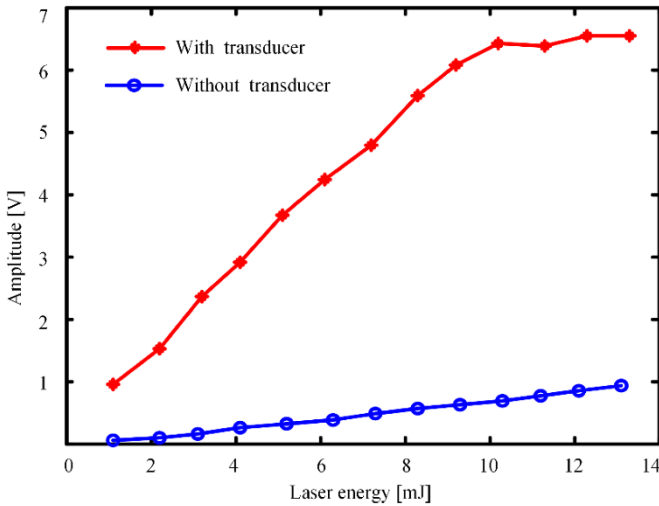

Figure 11. Peak-to-peak amplitudes of longitudinal wave signals excited under various laser energy with and without using the laser ultrasound transducer.

group velocity of 3.138 mm μs^{-1}. According to the dispersion curve of the A_0 mode, the group velocity at 647 kHz is 3.177 mm μs^{-1}. The error between the measured velocity and the theoretical value is 1.22%, proving the successful excitation of the pure A_0 mode. In figure 12(b), multiple wave packets appear, wherein the group velocity of the first wave packet is 5.311 mm μs^{-1}, which is similar to the group velocity of the 647 kHz S_0 mode (5.236 mm μs^{-1}). The measured group velocities have a variance within 0.5%.

The reason for the subsequent wave packets lie in the reflections of the incident wave within the transducer. After the incident wave reflects at the interface between the transducer and the metal plate, it could reflect again at the oblique surface of the wedge and reach the interface with a double incident angle, thereby exciting other low-speed modes. More specifically, when the incident longitudinal wave reaches the transducer-plate interface again, as shown in figure 13, the incident angle becomes the triple of the first incident wave ($\theta_2 = 3\theta_1$). As the critical angle of the S_0 mode is so small that

the incident angle of the secondary incident wave still falls in the critical angle domain of the A_0 mode, the Lamb wave of A_0 mode will be excited. However, the critical angle of excitation for A_0 mode is large, and the angle of secondary incidence exceeds the critical angle of other modes. Therefore, no other modes can be contained in the A_0 wave packet.

Through the amplitude comparison, it can be seen that the peak-to-peak value of the signal of the A_0 mode (1.62 V) is larger than that of the S_0 mode signal (0.808 V). The time pulse width (8.78 μs) of the A_0 mode time domain signal is significantly narrower than the S_0 modal signal (11.64 μs), suggesting a higher imaging resolution. Therefore, based on the comparison between the above experimental results, the A_0 mode Lamb wave can meet the requirement for the single mode excitation and is used in subsequent imaging experiments.

4.3. Defect detection with the laser ultrasound transducer

For the experimental data processing, the scanning areas are discretized within the polar coordinates (r, φ). The distances between the interested point with the excitation position and with the receiving element are calculated and converted into the time delays according to the group velocity of the guide wave. Based on the SAFT method, the defect reflection signal strength can be obtained at that point. The half-plane scanning image is shown in figure 14. The regions with the brightest color represent the higher amplitude reflected echoes which occur around the defects. It can be seen that the defect position is in the direction of 93° and with the radial position of 162 mm. It is close to the actual position of the defect on the test sample ($r = 160$ mm and $\varphi = 92°$) with the error down to 1.07%, indicating that the above synthetic aperture imaging results could locate the defect accurately.

In addition, there are other bright areas on the same circumference of the defect center. This can be attributed to the grating lobe of the piezoelectric sensing array and the insufficient signal-to-noise ratio due to the limited number of the array elements. Nevertheless, the amplitudes of these areas are much
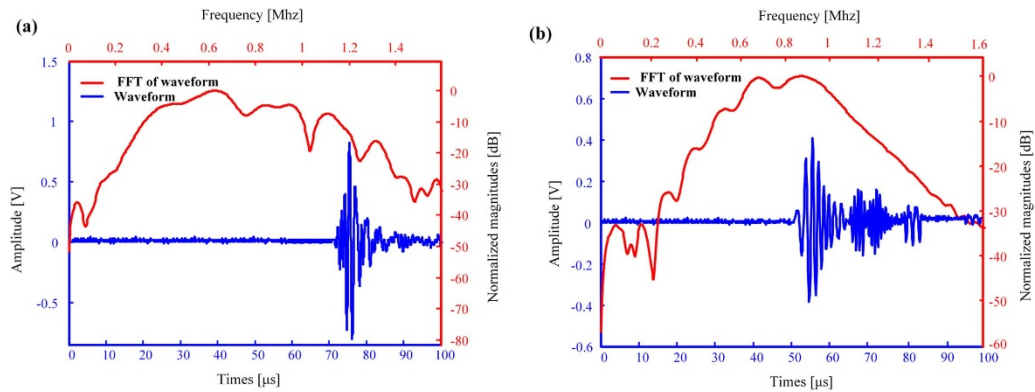
Figure 12. The performance of the wedge-shaped laser ultrasound transducer for exciting the Lamb wave. (a) A0 mode. (b) S0 mode.
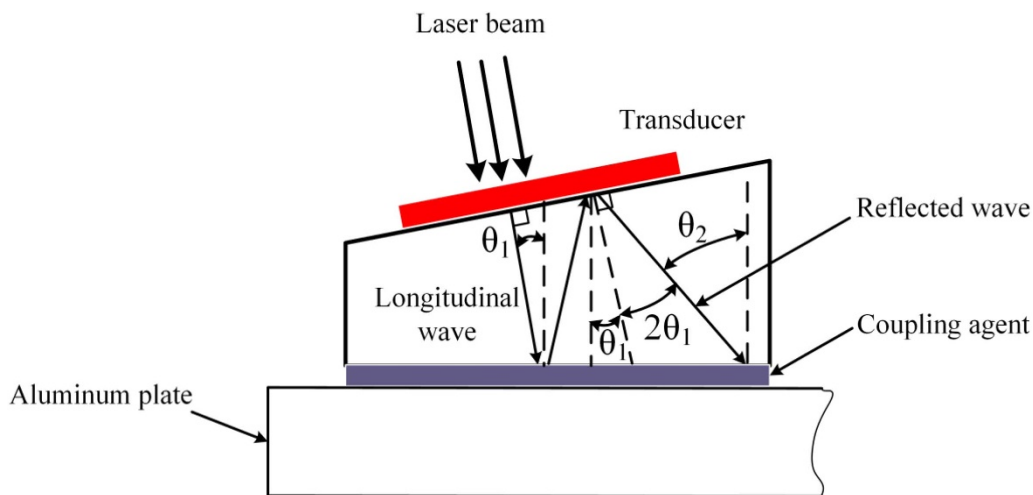

Figure 13. Schematic diagram of the secondary reflection in the wedge.

lower (within 10 dB) compared with that of the real defect location (20 dB). This phenomenon can be suppressed by using a denser piezoelectric array distribution and a larger synthetic aperture.

4.4. Benefits of the laser ultrasound transducer

Quite a few studies have shown that the application of narrow band Lamb wave is favorable for limiting the dispersion phenomenon. When using a piezoelectric transducer, a specific dimension is selected for exciting a single mode and low dispersive Lamb wave, as the piezoelectric transducer can only excite the Lamb wave at its resonance frequency. However, in some scenarios, multiple modes are preferred to examine subtler details of the structure, thus requiring a wideband excitation capability for the transducer [33–35]. The proposed transducer herein can be more suitable for such demand than the traditional piezoelectric transducer.

Moreover, traditional wedge transducers that use a piezoelectric contact transducer rely on the acrylic wedge as an intermediate between the transducers and the substrate to generate Lamb waves in the substrate. The large difference in acoustic impedance between the wedge and the piezoelectric transducer results in large reflection coefficients, hence

the reduced detection sensitivity. In contrast, the proposed CSNPs-PDMS transducer used a PDMS wedge, which has a similar material property as the transducer. Therefore, the design of the transducer can be greatly simplified, without considering the complex backing and matching layers. Moreover, the CSNPs-PDMS material is low cost and easy to fabricate, and thus can be applied to a structure on a large scale by using the approach like spraying and pasting. The flexible nature of the CSNPs-PDMS material makes it appropriate for examining the structure with complex geometry. In addition, attributed to the non-contact nature of the laser excitation, it eliminates the bulky wiring of the piezoelectric actuating nodes. Lastly, the immunity to the electromagnetic interference allows its application for some extreme cases.

5. Conclusion

In this paper, a flexible laser ultrasound transducer is designed to excite Lamb waves and apply them to defect detection in aluminum panels. Comparing to the performance of the conventional laser ultrasound technique for the longitudinal wave excitation in a 1.5 mm thick aluminum plate, it is found that the proposed transducer could generate an acoustic wave with
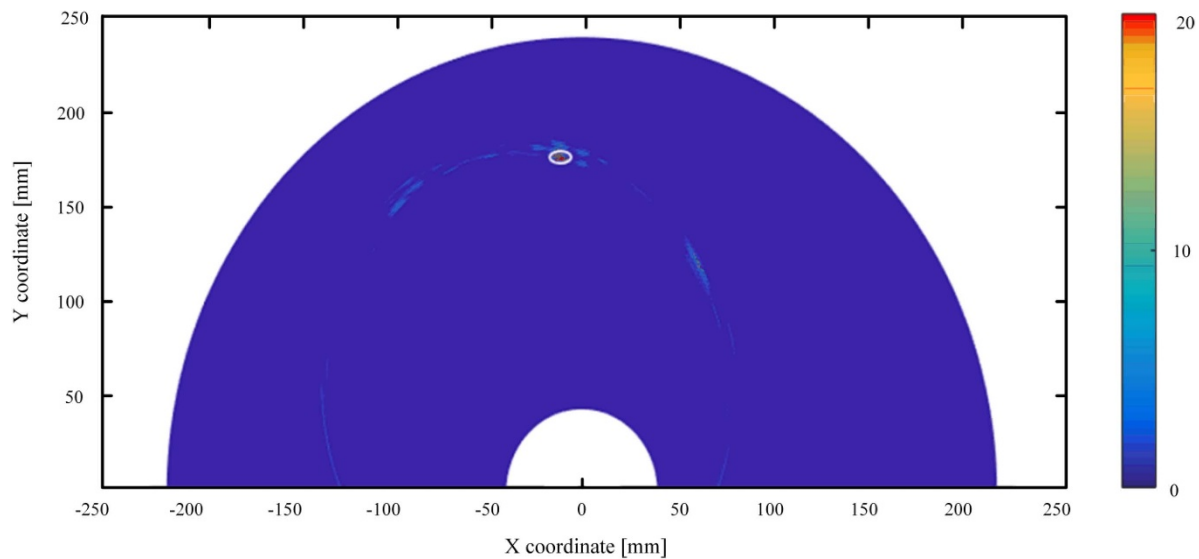
Figure 14. The scanning image by the laser ultrasound transmitter and piezoelectric receiver array system (shown on 20 dB logarithmic scale).

a 10 times amplitude magnification, proving the high photoacoustic conversion efficiency of the transducer. The laser ultrasonic transducer was further used to excite the Lamb wave signal of a single A_0 mode by oblique incidence, which indicates that the interference of other modal signals can be effectively avoided in actual application. Finally, the 1D linear array piezoelectric sensor is used to receive the reflected defect signal. According to the principle of synthetic aperture focusing imaging, the Lamb wave successfully locates the defect of the aluminum plate. It is verified that Lamb wave excitation based on this new laser ultrasonic transducer is feasible for SHM.

Acknowledgments

ORCID iDs

Yanfeng Shen ⬛ https://orcid.org/0000-0002-3025-4664
Wenbin Huang ⬛ https://orcid.org/0000-0002-5422-6481

References

[1] Mitra M and Gopalakrishnan S 2016 Guided wave based structural health monitoring: A review *Smart Mater. Struct.* **25** 53001

[2] Wang L and Yuan F G 2007 Group velocity and characteristic wave curves of Lamb waves in composites: modeling and experiments *Compos. Sci. Technol.* **67** 1370–84

[3] Su Z and Ye L 2009 *Identification of Damage Using Lamb Waves: From Fundamentals to Applications* (Berlin: Springer) (https://doi.org/10.1007/978-1-84882-784-4)

[4] Senyurek V Y 2015 Detection of cuts and impact damage at the aircraft wing slat by using Lamb wave method *Measurement* **67** 10–23

[5] Rucka M, Zima B and Kędra R 2014 Application of guided wave propagation in diagnostics of steel bridge components *Arch. Civ. Eng.* **60** 493–516

[6] Silk M G 1984 *Ultrasonic Transducers for Nondestructive Testing* (Amsterdam: Elsevier) (https://doi.org/10.1016/0308-9126(85)90093-8)

[7] Dewhurst R J, Edwards C E, McKie A D W and Palmer S B 1987 Comparative study of wide-band ultrasonic transducers *Ultrasonics* **25** 315–21

[8] Kobayashi M and Jen C-K 2004 Piezoelectric thick bismuth titanate/PZT composite film transducers for smart NDE of metals *Smart Mater. Struct.* **13** 951–6

[9] Khalili P and Cawley P 2018 Relative ability of wedge-coupled piezoelectric and meander coil EMAT probes to generate single-mode Lamb waves *IEEE Trans. Ultrason. Ferroelectr. Freq. Control* **65** 648–56

[10] Ribichini R, Cegla F, Nagy P B and Cawley P 2011 Study and comparison of different EMAT configurations for SH wave inspection *IEEE Trans. Ultrason. Ferroelectr. Freq. Control* **58** 2571–81

[11] Liu Z, Chen H, Sun K, He C and Wu B 2018 Full non-contact laser-based Lamb waves phased array inspection of aluminum plate *J. Vis.* **21** 751–61

[12] Lee S E, Liu P, Ko Y W, Sohn H, Park B and Hong J-W 2019 Study on effect of laser-induced ablation for Lamb waves in a thin plate *Ultrasonics* **91** 121–8

[13] Kim J, Kim H W, Chang W Y, Huang W, Jiang X and Dayton P 2019 Candle-soot carbon nanoparticles in photoacoustics: advantages and challenges for laser ultrasound transmitters *IEEE Nanotechnol. Mag.* **13** 13–28

[14] Chen S-L 2016 Review of laser-generated ultrasound transmitters and their applications to all-optical ultrasound transducers and imaging *Appl. Sci.* **7** 25

[15] Colchester R J *et al* 2019 All-optical rotational ultrasound imaging *Sci. Rep.* **9** 1–8

[16] Noimark S *et al* 2016 Carbon-nanotube–PDMS composite coatings on optical fibers for all-optical ultrasound imaging *Adv. Funct. Mater.* **26** 8390–6

[17] Rose J L 2014 *Ultrasonic Guided Waves in Solid Media* (Cambridge: Cambridge University Press) (https://doi.org/10.1017/CBO9781107273610)

[18] Harb M S and Yuan F G 2015 Lamb wave dispersion and anisotropy profiling of composite plates via non-contact air-coupled and laser ultrasound *AIP Conf. Proc.* **1650** 1229–38

[19] McDonald F A and Wetsel G C Jr 1978 Generalized theory of the photoacoustic effect *J. Phys. D: Appl. Phys.* **49** 2313–22

[20] Huang W, Chang W-Y, Kim J, Li S, Huang S and Jiang X 2016 A novel laser ultrasound transducer using candle soot carbon nanoparticles *IEEE Trans. Nanotechnol.* **15** 395–401

[21] Paltauf G and Dyer P E 2003 Photomechanical processes and effects in ablation *Chem. Rev.* **103** 487–518

[22] Mohammadzadeh M, Gonzalez-Avila S R, Wan Y C, Wang X, Zheng H and Ohl C-D 2016 Photoacoustic shock wave emission and cavitation from structured optical fiber tips *Appl. Phys. Lett.* **108** 24101

[23] Xu M and Wang L V 2006 Photoacoustic imaging in biomedicine *Rev. Sci. Instrum.* **77** 41101

[24] Lee T, Baac H W, Ok J G and Jay Guo L 2018 Polymer–nanomaterial composites for optoacoustic Conversion Functional Organic and Hybrid Nanostructured Materials: Fabrication, Properties, and Applications (Weinheim: Wiley) ch 14 (https://doi.org/10.1002/9783527807369.ch14)

[25] Hsieh B-Y, Kim J, Zhu J, Li S, Zhang X and Jiang X 2015 A laser ultrasound transducer using carbon nanofibers–polydimethylsiloxane composite thin film *Appl. Phys. Lett.* **106** 21902

[26] Hou Y, Ashkenazi S, Huang S-W and O'Donnell M 2008 An integrated optoacoustic transducer combining etalon and black PDMS structures *IEEE Trans. Ultrason. Ferroelectr. Freq. Control* **55** 2719–25

[27] Chang W-Y, Huang W, Kim J, Li S and Jiang X 2015 Candle soot nanoparticles-polydimethylsiloxane composites for laser ultrasound transducers *Appl. Phys. Lett.* **107** 161903

[28] Baac H W *et al* 2012 Carbon-nanotube optoacoustic lens for focused ultrasound generation and high-precision targeted therapy *Sci. Rep.* **2** 989

[29] Che J, Cagin T and Goddard W A III 2000 Thermal conductivity of carbon nanotubes *Nanotechnology* **11** 65

[30] Sicard R, Goyette J and Zellouf D 2002 A SAFT algorithm for lamb wave imaging of isotropic plate-like structures *Ultrasonics* **39** 487–94

[31] Davies J and Cawley P 2009 The application of synthetic focusing for imaging crack-like defects in pipelines using guided waves *IEEE Trans. Ultrason. Ferroelectr. Freq. Control* **56** 759–71

[32] Wu J N, Ling Y and Wang J J 2017 A novel denoising algorithm for acceleration signal based on compressed sensing *Proc. 13th Int. Conf. on Natural Computation, Fuzzy Systems and Knowledge Discovery (ICNC-FSKD)* pp 900–4 (https://doi.org/10.1109/FSKD.2017.8393396)

[33] Terrien N, Osmont D and Royer D 2007 A combined finite element and modal decomposition method to study the interaction of Lamb modes with microdefects *Ultrasonics* **46** 74–88

[34] Michaels J E, Lee S J, Croxford A J and Wilcox P D 2013 Chirp excitation of ultrasonic guided waves *Ultrasonics* **53** 265–70

[35] Michaels J E, Lee S J, Hall J S and Michaels T E 2011 Multi-mode and multi-frequency guided wave imaging via chirp excitations *Proc. SPIE* **7984** 79840I